MTR 03B0000075

MITRE TECHNICAL REPORT

Finite Sampling Considerations for GMTI STAP and Sensor Modeling

September 2003

T. P. Guella
B. N. Suresh Babu

Sponsor: ESC
Dept. No.: D710, D720
Contract No.: F19628-99-C-0001
Project No.: 03035518-CC

MITRE
Center for Air Force C2 Systems
Bedford, Massachusetts

MITRE Department Approval:

S. B. Bowling

MITRE Project Approval:

B. N. Suresh Babu

Abstract

The continuing objectives of Project 5518 are to develop and enhance the simulation capabilities for evaluating advanced modular sensor designs such as MP-RTIP and Global Hawk. The use of reduced subspace Space Time Adaptive Processing (STAP) architectures increases the probability of detection and improves the minimum detectable velocity (MDV). References [1, 2] discuss the details of earlier steady state performance evaluation for a Global Hawk weight compliant system using these architectures. This report will present the effects of finite sampling on system performance using the properties of the Wishart distribution and will present a method by which some of the finite sample losses may be recovered through subaperture processing to improve the performance.

Acknowledgments

The authors would like to acknowledge Joseph B. Gaffney for providing an earlier version of the MATLAB Code used in the analysis.

Table of Contents

List of Figures

List of Tables

Section 1

Introduction

The continuing objectives of Project 5518 are to develop and enhance the simulation capabilities for evaluating advanced modular sensor designs such as MP-RTIP and Global Hawk. The use of reduced subspace STAP architectures increases the probability of detection and improves the minimum detectable velocity (MDV). References [1, 2] discuss the details of earlier steady state performance evaluation for a Global Hawk weight compliant system using these architectures. This report will present the effects of finite sampling on system performance using the properties of the Wishart distribution and will present a method by which some of the finite sample losses may be recovered through subaperture processing to improve the performance.

Estimation of the complex interference environment and the subsequent estimation of the adaptive weights is needed to evaluate the finite sample performance with different space time adaptive processing architectures. A computationally efficient and reasonably accurate way of evaluating the effects of finite sample losses is needed to evaluate the system performance. For systems with large degree-of-freedom (DOF) dimensionality, straightforward averaging of covariances from large sets of training range bins can quickly become a computational bottleneck when estimation of the adaptive weights are needed over many target cells. The use of the Wishart Distribution provides a means of quickly calculating a sample covariance matrix corresponding to any number of samples greater than the DOF dimension. The time taken to form an estimate by means of the Wishart distribution is essentially independent of the number of range samples, so that a quick evaluation of finite sample loss effects on the system performance can be efficiently evaluated. The use of the Wishart distribution in determining the covariance estimate assumes stationary Gaussian distributed noise-only data vectors for the estimation process.

That is, the noise data are assumed to be N dimensional complex Gaussian vectors of zero mean and covariance **R,** where N denotes the number of adaptive degrees of freedom (DOF).

New methods are needed for covariance matrix estimation when the environment becomes sample-limited. By sample-limited we mean cases when it is difficult to find a training set large enough to support an estimate of the covariance matrix. This shortcoming can arise from a number of reasons, notably when the target encompasses many range bins and thereby excludes these bins from being included in the training set. Also, when the interference environment is only short term stationary over range, the number of training cells that share the same statistics of the target cell can be limited. One solution around this problem is the inclusion of enhanced spatial sampling by means of subaperture averaging. [6, 7]. This procedure uses a reduced dimension subaperture of the full aperture that is incrementally progressed along the full array. Covariance matrices are calculated for each subaperture and subsequently averaged. The procedure is repeated for each range bin in the training set. The procedure therefore produces a multiplicative increase in the sample support at the expense of using a smaller spatial aperture in place of a larger full aperture. If the subaperture is only slightly smaller than the full aperture, the enhancement gained by the larger sample support quickly outweighs the losses attributed to using the smaller aperture.

In this report we will employ a notional UAV X-Band radar example [1, 2] to evaluate the impact on system performance due to finite sampling effects. In addition, this report introduces subaperture averaging to improve the performance when the sample size is small relative to system dimensionality.

This report is organized as follows. Section 1 briefly discusses STAP and the details of the complex Wishart distribution; section 2 describes the subaperture averaging method and section 3 summarizes the results.

1.1 Space Time Adaptive Processing

Space Time Adaptive Processing (STAP) refers to the application of adaptive techniques that simultaneously combine the signals received by multiple antenna elements (the spatial domain) at each pulse repetition interval (the temporal domain) of a coherent processing interval. This report focuses on one suboptimal reduced dimension STAP architecture, namely the factored time-space (FTS) or Doppler factored STAP architecture. The time-space factored STAP Doppler processes first, and then adaptively combines the elements in each Doppler bin. Higher order time-space factored STAP architectures use adjacent Doppler bins for temporal diversity. Details of the algorithms used in this report can be found in [8]. This report introduces the effects of using an estimated covariance matrix on system performance and compares the performance with the steady state case for a notional X-Band UAV radar. The report makes use of the complex Wishart distribution as a means of quickly evaluating the losses incurred by estimating the covariance matrix. The results from the Wishart distribution are compared with results from conventional range bin averaging of the data, and it is shown that the two ways of modeling finite sample losses are equivalent.

The report also addresses the problem of having to estimate a covariance matrix when the number of range samples available for estimation falls short of the number needed. It is well known that for a system possessing N degrees of freedom (DOF), roughly 2N samples are needed for an expected loss of 3 dB with 5N samples necessary for an expected loss of 1 dB in system performance. Generally, real systems require somewhere between 3N and 5N samples for estimation to maintain performance. This report introduces the technique of subaperture averaging to address this problem. The details of this method as applied to the notional X-Band UAV radar are presented in section 2 of this report.

1.2 Complex Wishart Distribution Applied to the Finite Sampling Problem

The method of factorization of the complex Wishart distribution which follows is based on the derivation given by J. Capon and N. R. Goodman [3, 4]. The sample covariance matrix obtained from K samples of the noise environment is given by the well known formula

$$\hat{\mathrm{R}} = \frac{1}{\mathrm{K}} \sum_{\mathrm{k}=1}^{\mathrm{K}} \vec{\mathrm{r}}_{\mathrm{k}} \vec{\mathrm{r}}_{\mathrm{k}}^{\mathrm{H}} \tag{1}$$

which is the maximum likelihood estimator for the covariance matrix **R**. The vector $\vec{\mathbf{r}}_{\mathbf{k}}$ is the complex noise data vector for the k^{th} sample and superscript H denotes the Hermitian conjugate vector. If the $\vec{\mathbf{r}}_{\mathbf{k}}$ are assumed to be N dimensional complex Gaussian vectors of zero mean and covariance **R**, and if K ≥ N, then the probability distribution of the elements of the sample covariance matrix $\hat{\mathbf{R}}$ is completely specified by the complex Wishart distribution. If we let **A** = K**R** then the joint probability density function of the elements of **A** may be written as

$$\sigma_{\mathrm{K,N}}^{(\mathrm{A})} = \frac{\left|\mathrm{A}\right|^{\mathrm{K-N}} \left|\mathrm{R}\right|^{-\mathrm{K}} \mathrm{e}^{-\mathrm{Tr}\left(\mathrm{R}^{-1}\mathrm{A}\right)}}{\pi^{\mathrm{N}(\mathrm{N}-1)/2}\, \Gamma(\mathrm{K}) \cdots \Gamma(\mathrm{K}-\mathrm{N}+1)} \tag{2}$$

where $\left|\cdots\right|$ denotes the determinant of the enclosed matrix, Tr denotes the trace and $\Gamma(\mathrm{k})$ denotes the gamma function.

$$\Gamma(\mathrm{k}) = (\mathrm{k}-1)! \tag{3}$$

The probability density function given by Equation (2) is defined over the domain of non-negative definite Hermitian matrices. The form of the distribution is not easy to use since in general the elements of the sample covariance matrix are not statistically independent so that the distribution does not factorize in any convenient way. A useful representation for numerical evaluation can be obtained for the distribution by first doing a Cholesky decomposition of the matrix **A.** For every positive definite Hermitian matrix, there exists a unique upper triangular matrix **U** such that

$$A = U^H U \tag{4}$$

where **U** is a N × N matrix composed of unrestricted entries above the main diagonal, real entries along the main diagonal and zeros elsewhere. Goodman [3] has shown that the joint probability distribution function of the elements of **U** is generally of the form

$$\sigma_{K,N}^{(U)} = \frac{2^N \left|R\right|^{-K} \prod_{n=1}^{N} u_{nn}^{2K-(2n-1)} \; e^{-Tr(R^{-1}U^H U)}}{\pi^{N(N-1)/2}\Gamma(K)\cdots\Gamma(K-N+1)} \tag{5}$$

When **R** is the identity matrix **I** the joint probability distribution function of the elements of **U** simplifies to

$$\sigma_{K,N}^{(U)} = \frac{2^N \prod_{n=1}^{N} u_{nn}^{2K-(2n-1)} \; e^{-\sum_{mn}\left|u_{mn}\right|^2}}{\pi^{N(N-1)/2}\Gamma(K)\cdots\Gamma(K-N+1)} \tag{6}$$

The probability distribution given in Equation (6) can now be written as the product of N + N(N-1)/2 terms, with each term in the product being a function of a single random variable u_{mn}. The part of this probability distribution corresponding to the off-diagonal terms u_{mn} of **U** for m<n, describes the probability distributions of complex Gaussian random variables with zero mean and unit variance. If the N(N-1)/2 complex Gaussian terms are integrated out from the above expression, what is left is the joint probability distribution of the main diagonal terms of **U,**

$$\sigma_{K,N}\left(u_{11},u_{22},\ldots,u_{NN}\right)=\prod_{n=1}^{N}\frac{2u_{mn}^{2K-(2n-1)}}{\Gamma\left(K-n+1\right)}e^{-u_{mn}^{2}} \tag{7}$$

The n^{th} diagonal term of the above equation has the marginal density

$$\sigma_{K,N}^{(u_{mn})}=\frac{2}{\Gamma\left(K-n+1\right)}u_{nn}^{2(K-n+1)-1}\,e^{-u_{nn}^{2}} \tag{8}$$

for $u_{nn} > 0$. The probability distribution given above is closely related to the chi-square distribution with 2(K-n+1) degrees of freedom. If a change of variables is made such that

$$\gamma_n = u_{nn}^2 \tag{9}$$

a simple scaling of a chi-square random variate with 2n degrees of freedom is affected. The change of variables shows that the diagonal elements of the matrix U are seen to be square roots of integer order gamma variates. Thus, the evaluation of the sample covariance matrix by means of the complex Wishart distribution can be reduced to the evaluation of Gaussian distributed variates for the off-diagonal terms and gamma distributed variates for the main diagonal terms.

A statement about computational efficiency is appropriate since the reason for implementing the Wishart distribution to simulate finite sample loss effects is based on computational advantage. To compute the sample covariance by directly calculating the average covariance over K range gates requires KN(N+1)/2 complex multiplications, so that the computational burden is roughly KN^2. In contrast, the computational work required by using the Wishart distribution amounts to doing a complex Cholesky decomposition, calculating the gamma and Gaussian variates and doing the final matrix multiplication to obtain $\hat{\mathbf{R}}$. This is roughly proportional to N.

1.3 Numerical Evaluation of Sample Covariance Matrix

Let **R** be the steady state covariance matrix derived from the phenomenological models portrayed in a computer simulation. The sample covariance matrix $\hat{\mathbf{R}}$ based on K observations can be determined from the Wishart distribution using the following method, which is based on the previous section's factorization method. We note that to insure that the covariance matrix is nonsingular, we require that $K \geq N$ where N is the dimensionality of the matrix **R**. We first factor **R** into its Cholesky decomposition as

$$\mathbf{R} = \mathbf{C}^{\mathbf{H}}\mathbf{C} \tag{10}$$

We now note that any data vector $\vec{\mathbf{r}}_k$ that is complex Gaussian distributed with covariance R may be written as

$$\vec{\mathbf{r}} = \mathbf{C}^{\mathbf{H}}\vec{\mathbf{w}} \tag{11}$$

where $\vec{\mathbf{w}}$ is a unit variance, zero mean complex Gaussian variate. The above can be seen to be true as follows,

$$\begin{aligned}\left\langle \vec{\mathbf{r}}\vec{\mathbf{r}}^{\mathbf{H}} \right\rangle &= \left\langle \mathbf{C}^{\mathbf{H}}\vec{\mathbf{w}}\left(\mathbf{C}^{\mathbf{H}}\vec{\mathbf{w}}\right)^{\mathbf{H}} \right\rangle \\ &= \mathbf{C}^{\mathbf{H}}\left\langle \vec{\mathbf{w}}\vec{\mathbf{w}}^{\mathbf{H}} \right\rangle \mathbf{C} \\ &= \mathbf{C}^{\mathbf{H}}\mathbf{I}\mathbf{C} = \mathbf{R}\end{aligned} \tag{12}$$

Thus, an arbitrary sample covariance matrix of $\vec{\mathbf{r}}$ is statistically equivalent to a linear transformation of a corresponding sample covariance matrix of $\vec{\mathbf{w}}$ by virtue of the fact that $\left\langle \vec{\mathbf{w}}\vec{\mathbf{w}}^{\mathbf{H}} \right\rangle = \mathbf{I}$. If we denote the sample covariance matrix of $\vec{\mathbf{w}}$ by

$$\hat{\mathbf{W}} = \vec{\mathbf{w}}\vec{\mathbf{w}}^{\mathbf{H}} \tag{13}$$

and now take the Cholesky decomposition of the matrix $\mathbf{K}\hat{\mathbf{W}}$

$$\mathbf{K}\hat{\mathbf{W}} = \mathbf{U}^{\mathbf{H}}\mathbf{U} \tag{14}$$

From the analysis described in Section 1.2, the elements of the upper triangular matrix **U** will be statistically independent. Also, the nonzero off-diagonal elements of **U** will be complex Gaussian variates with zero mean and unit variance and the main diagonal entries will be square roots of integer order gamma variates with a form factor proportional to the sample size K. Once the sample covariance matrix $\hat{\mathbf{W}}$ for the normalized Gaussian variates is computed, the transformation

$$\hat{\mathbf{R}} = \mathbf{C}^{\mathbf{H}}\hat{\mathbf{W}}\mathbf{C} \tag{15}$$

is then performed to obtain the desired sample covariance matrix $\hat{\mathbf{R}}$ based on K observations, for the steady state matrix **R.**

1.4 Finite Sample Performance for X-Band UAV Radar

Earlier, the Advanced Airborne Radar Simulation (AARS) was used to assess the performance of airborne X-Band UAV radar with different STAP architectures [1, 2]. Table 1 shows the system parameters used in the study.

Table 1. UAV Parameters for Non-Overlapped Array

Parameter	Value
Number of Antenna Elements	120 columns; 30 Rows
Center Frequency	10 GHz
Pulse Repetition Frequency	2.0 msec
LFM Bandwidth	15 MHz
LFM Uncompressed Pulsewidth	16.67 usec
Fractional Wavelength Spacing	0.508 for Columns; 0.678 for Rows
Clutter Model	Constant Sigma; Mean Level of -20 dB
Internal Clutter Motion	None
Number of PRIs	32
Number of Dopplers	32; Blackman Weighting
Transmit Aperture Weighting	Uniform in Azimuth and Elevation
Electronic Scanning	Broadside in Azimuth; 5.31 Degrees in Elevation
Number of Receive Azimuth Subarrays	12 (Non-Overlapping)
Number of Elevation Subarrays	1
Receive Subarray Aperture Weighting	Uniform in Azimuth and Elevation
Beamformer Weighting	60 dB Taylor (Transition Number = 4)
Transmit Power	20 KW
Platform Velocity	180 m/sec
Platform Altitude	45000 ft
Target RCS	10 sq meters
Element Pattern Type	Half Wavelength Dipole

The system has twelve spatial adaptive degrees of freedom. First- through third- order post factored time-space STAP (or Doppler-factored STAP) architectures were evaluated for their effectiveness in improving the minimum detectable velocity and probability of detection performance. Since first order factored STAP is an application of spatial adaptivity in each Doppler bin the number of adaptive degrees of freedom is twelve for this case. Second and third order factored STAP couple two and three adjacent Doppler bins, so the number of adaptive degrees of freedom increases to twenty-four and thirty- six, respectively. The steady state performance for the signal-plus-interference-to-noise ratio (SINR) as a function of Doppler is shown in Figure 1. The adaptive SINR results are compared with the non adaptive SINR. In Figures 2 and 3 we used a sample size of five times the number of adaptive DOF (180 samples) for the third order factored STAP architecture (the green curves). For first and second order factored STAP the ratio of the sample size to adaptive DOF was 15 and 7.5, respectively. Figure 2 shows the SINR as a function of Doppler as calculated from the Wishart distribution, while Figure 3 shows the SINR curves by averaging the covariance matrix over 180 range gates.

The comparison between the two methods for estimating the covariance matrix and calculating the SINR performance shows that the results are in close agreement. In particular, the expected performance of the third order FTS in the clutter-free region is about 1 dB below the steady-state performance. This is expected since third order FTS processing is performed with a sample support of five times its adaptive DOF.

Figures 4 and 5 show the results of the comparison between the two methods for a sample support of twice the adaptive degrees of freedom for third order FTS processing. Again the performance curves are very similar. For third order FTS the clutter free SINR is about 3 dB below the steady state value depicted in Figure 1, which is the expected result.

The time taken to compute the above results using the Wishart distribution typically takes a few minutes when run on a 1 GHz personal computer, no matter what the sample size is. In contrast, depending on the sample size, the same calculations can easily take a few hours to run using the same computer resources using conventional range bin averaging.

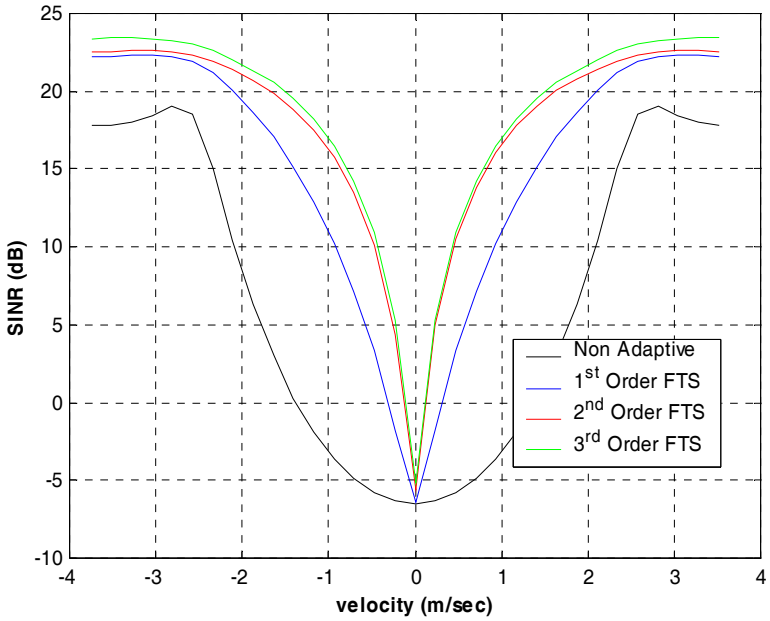

Figure 1. Steady-State Signal-to-Interference Ratio vs. Doppler

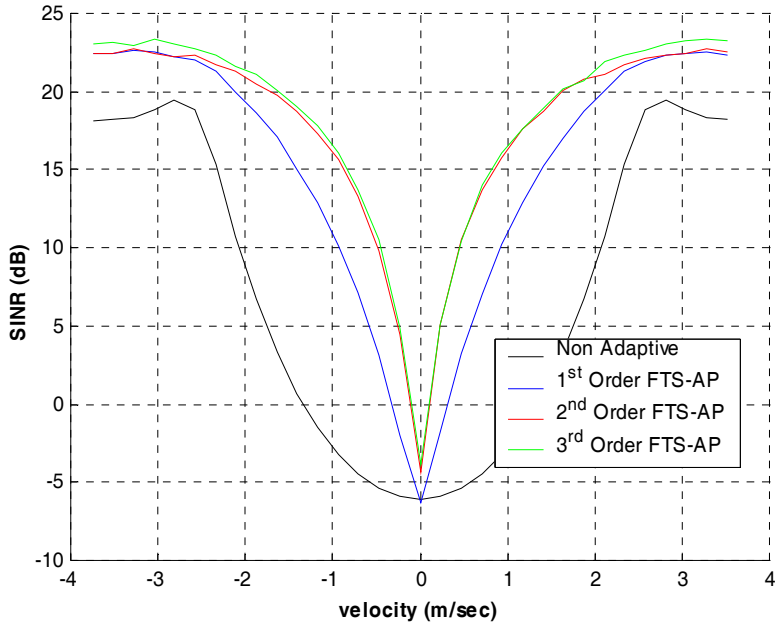

Figure 2. Finite Sample Signal-to-Interference Ratio vs. Doppler for 180 Sample Size Utilizing the Wishart Distribution

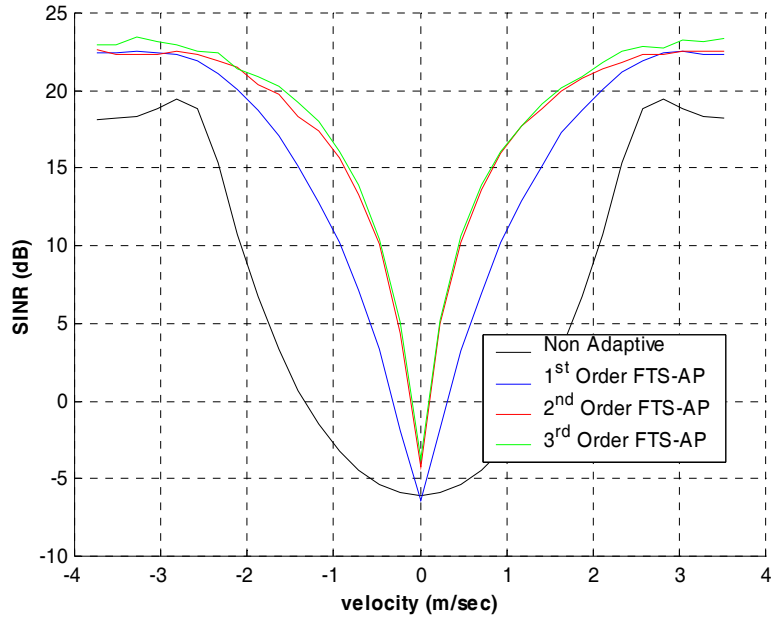

Figure 3. Finite Sample Signal-to-Interference Ratio vs. Doppler for 180 Sample Size Utilizing Range Gate Averaging

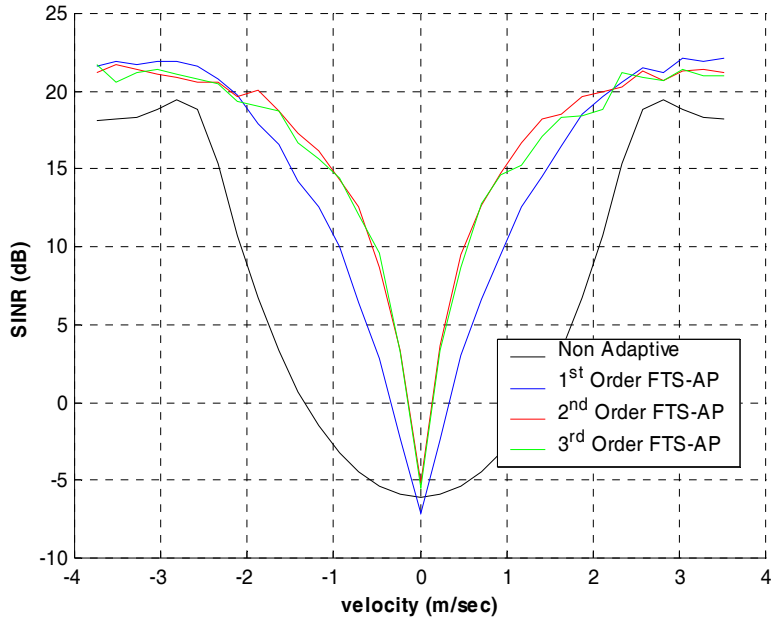

Figure 4. Finite Sample Signal-to-Interference Ratio vs. Doppler for 72 Sample Size Utilizing the Wishart Distribution

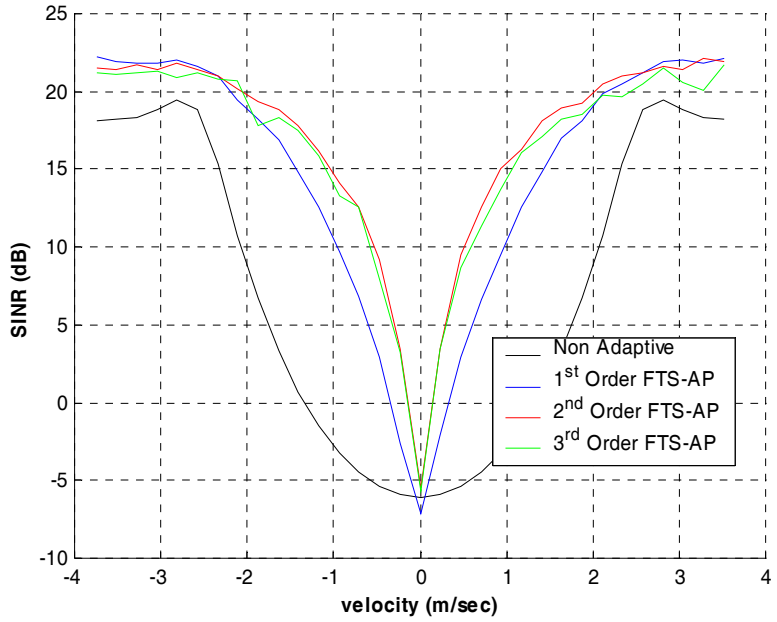

Figure 5. Finite Sample Signal-to-Interference Ratio vs. Doppler for 72 Sample Size Utilizing Range Gate Averaging

Section 2

Subaperture Averaging

2.1 Brief Overview

Subaperture averaging [6, 7] provides an efficient technique for increasing the effective averaging of the sample covariance matrix and can be readily applied if the antenna array is composed of identical elements. Figure 6 illustrates the idea behind subaperture averaging. For an array made up of N elements, a reduced dimension subaperture of L elements with $L < N$ is used to carry out the averaging procedure. Starting from one side of the full aperture N element array the subaperture samples the incoming wavefront at element locations 1 through L. The subaperture is then progressed by one element and samples of the incoming wavefront are taken for elements 2 through L+1. This incremental sampling of the wavefront is continued until the sliding subaperture of L elements has been translated to the other side of the full aperture of N elements. Subaperture motion from left to right produces what is generally termed forward averaging. The subaperture-generated L x L sample covariance matrix is given by

$$\hat{R}_f = \frac{1}{K(N-L+1)} \sum_{k=1}^{K} \sum_{i=1}^{N-L+1} \vec{r}(k)_i \, \vec{r}(k)_i^H \qquad (16)$$

where K is the number of range cells and $\vec{r}(k)_i$ is the segment of the data vector from the k^{th} range spanning elements i through (N-L+1) of the full aperture. The subscript f for the estimated subaperture covariance matrix denotes the fact that this is the covariance matrix by forward (left to right) progression of the subaperture along the full aperture. The averaging can in fact be doubled by reversing the progression of the subaperture and performing the same procedure from right to left. This subaperture motion from right to left produces what

is known as ‘reversed’ or ‘backward’ subaperture averaging. The combined average covariance matrix generated by employing both forward and backward subaperture averaging is given by

$$\hat{R}_{fb} = \frac{\left(\hat{R}_f + \hat{R}_b\right)}{2} \tag{17}$$

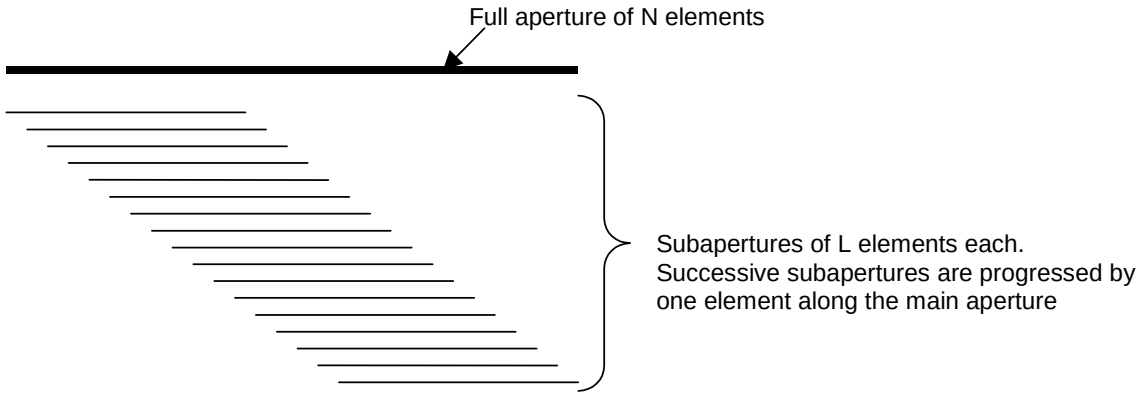

Figure 6. Illustration of Subaperture Averaging Procedure

The idea behind subaperture averaging is that for an array of evenly spaced identical elements the steady state covariance matrix is Toeplitz, which means that elements along any diagonal of the matrix are equal. When the covariance matrix is estimated the Toeplitz nature of the matrix is lost. As more samples are added to the estimation process the estimates of the entries along the diagonals of the matrix are ‘smoothed out’ and approach the Toeplitz steady state covariance matrix . Subaperture averaging provides for a smoothing out of the entries of the covariance matrix of the subaperture. The basic mechanism of the smoothing is realized with the recognition that the estimate of the mn^{th} entry of the matrix for elements m and n is effectively repeated in the $(m+q)(n+q)^{th}$ entry, where q is an integer, as

long as the array elements are identical and equally spaced, that is as long as the array satisfies the Toeplitz conditionality. The subarray covariance matrices are the diagonally centered submatrices of the full aperture $N \times N$ covariance matrix.

The subaperture averaging method used in this study is a extension of the algorithm described in [5, 6] and employs subarrays. The case considered here was an array composed of non overlapping contiguous subarrays. Also, for second and third order FTS STAP processing, the covariance matrices span two and three Dopplers, respectively. This introduces a complication into the averaging procedure since the covariance matrix is no longer Toeplitz, except for the submatrices centered on the diagonal of the full matrix which span only one Doppler. The effect of using a non-Toeplitz covariance matrix can be seen in the SINR results presented later in this section.. For first order FTS processing, the improvement from applying subaperture averaging the covariance matrix spans only one Doppler. In this case, the steady state covariance matrix is Toeplitz and the benefit of subaperture averaging is realized. For second and third order FTS processing our results show that the effect of using a covariance matrix which spans more than one Doppler produces a more shallow clutter notch. The filling in of the clutter notch becomes progressively more pronounced as higher order FTS processing is performed (see Figure 7). The clutter free SINR performance is however restored to the amount expected from the sample support enhancement provided by the averaging. For the cases where the covariance matrix spans more than one Doppler, subaperture averaging produces a sample covariance matrix which tends to become more Toeplitz in character as more samples are included.

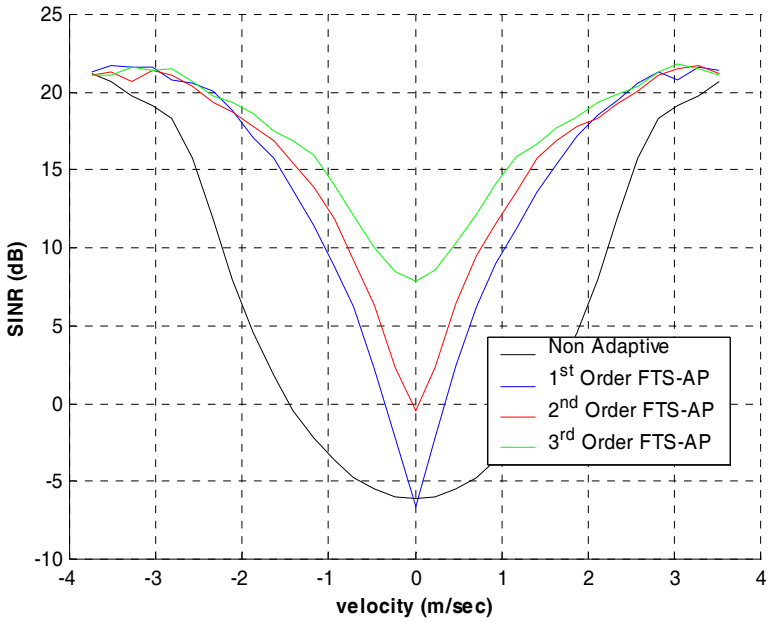

Figure 7. Finite Sample Signal-to-Interference Ratio vs. Doppler for 24 Range Samples Using Subaperture Averaging with a Subaperture Size of 10 Subarrays. Full Aperture Has 12 Subarrays

2.2 Subaperture Averaging Results

Figure 7 shows the SINR performance for 24 range samples using a subaperture size of 10 non overlapped subarrays. The full aperture is 12 subarrays long. The black curve is the steady state non adaptive SINR performance for the 10 subarray subaperture. The remaining three curves show the SINR performance for first through third order FTS processing. The sample support enhancement gained by using a subaperture size of 10 subarrays is a factor of three for each range sample. Thus, effectively 72 samples were used to estimate the covariance matrices for each of the three STAP architectures represented. For first order FTS, which has 10 adaptive DOF, the effective sample size is 7.2 times the adaptive DOF. For second order, the effective sample size is 3.6 times the adaptive DOF and for third order FTS the effective sample size is 2.4 times the adaptive DOF.

In contrast to Figure 7, Figure 8 shows the SINR performance for 24 range samples using no subaperture averaging. For second and third order FTS the number of range samples is less than that needed to insure the invertability of the covariance matrix. For these two cases a small amount of diagonal loading (-150 dB) was applied to make the covariance matrices positive definite and invertable. Clearly for this small sample size second and third order FTS cannot be evaluated. However, by using a slightly smaller aperture and implementing subaperture averaging, the SINR performance can be significantly improved. For first order FTS the number of samples available is twice the adaptive DOF. Figure 7 shows that by using a slightly smaller aperture and applying subaperture averaging, FTS performance can be made nearly optimal. Figures 9 and 10 show similar results for a sample size of 36 range bins for the 10 subarray subaperture with subaperture averaging.

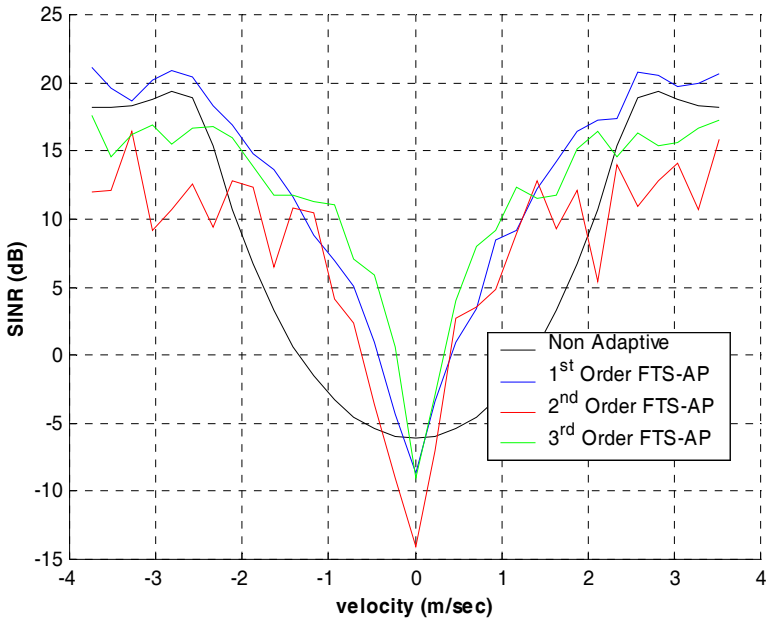

Figure 8. Finite Sample Signal-to-Interference Ratio vs. Doppler for 24 Range Samples for Full Aperture of 12 Subarrays

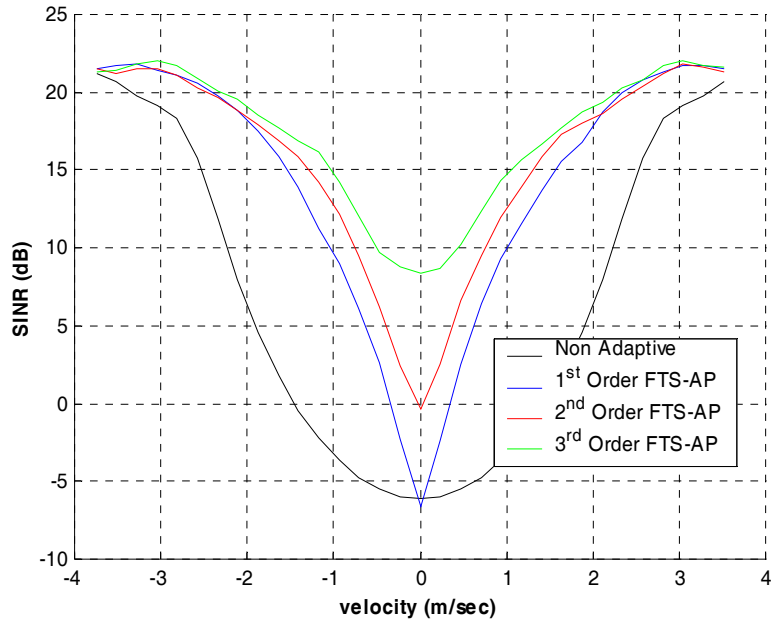

Figure 9. Finite Sample Signal-to-Interference Ratio vs. Doppler for 36 Range Samples Using Subaperture Averaging with a Subaperture Size of 10 Subarrays. Full Aperture Has 12 Subarrays

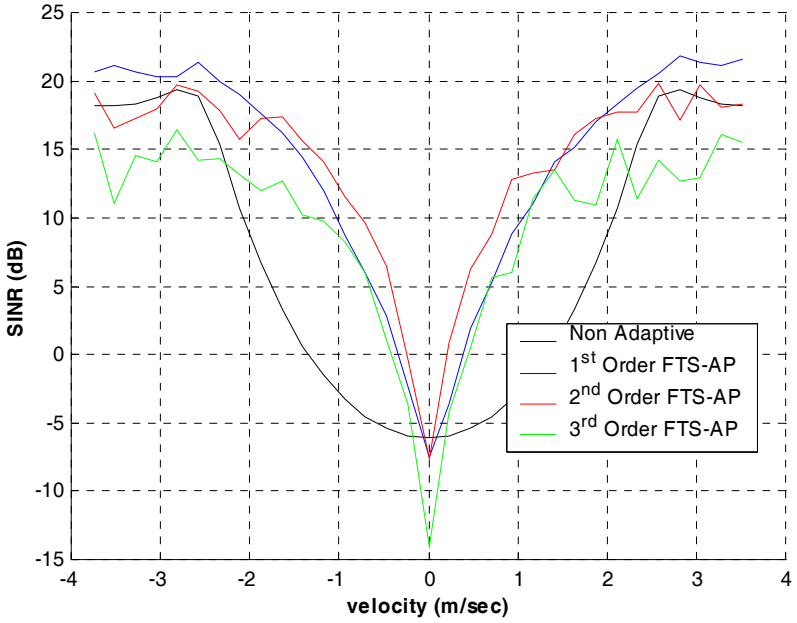

Figure 10. Finite Sample Signal-to-Interference Ratio vs. Doppler for 36 Range for Full Aperture of 12 Subarrays

Section 3

Conclusions

In the previous study [2], we have generated performance estimates for the weight compliant Global Hawk MP-RTIP platform. Performance is determined by generating the antenna patterns, the expected SINR, both before and after STAP, minimum detectable velocity and the expected ability of the system to detect targets. The results there were based on steady state performance.

In this report, the Advanced Airborne Radar Simulation was used to evaluate the performance of a notional UAV X-Band radar with STAP architectures with finite sampling effects included. We have added Wishart Sampling capability to the Advanced Radar Simulation (AARS) suite of analytical tools. This feature now enables quick assessment within AARS of finite sampling losses in radar performance and provides a means of comparison with steady state performance. It is important to note that the time taken to compute results using the Wishart distribution typically takes a few minutes, no matter what the sample size is. In contrast, depending on the sample size, the same calculations can easily take a few hours to run using the same computer resources.

In addition, we introduced the subaperture averaging method for estimation of the covariance matrix when the environment becomes sample-limited. We applied the technique of subaperture averaging to an array made up of evenly spaced identical subarrays. We also applied subaperture averaging to covariance matrices associated with higher order factored time-space processing (FTS), also known as Doppler factored STAP.

These two newly added capabilities were applied to a notional airborne X-Band UAV radar that has been modeled in previous work [1, 2]. The techniques described in this report were applied to evaluate the finite sample performance estimates for the weight compliant

Global Hawk MP-RTIP platform. The classified finite performance results were also completed for the weight compliant Global Hawk System with different STAP architectures but are not presented in this report. The results are documented in a classified addendum.

List of References

1. J. B. Gaffney, T. P. Guella, B. N. Suresh Babu, J. A. Torres, and H. B. Wollman, "GMTI STAP and Sensor Modeling," February 2000, The MITRE Corporation, Bedford, Massachusetts.

2. T. P. Guella, J. B. Gaffney, and B. N. Suresh Babu, "Analysis of the Performance of the Weight Compliant Global Hawk MP-RTIP Using a Non-Overlapped Contiguous Subarray Antenna (U)," March 2003, The MITRE Corporation, Bedford, Massachusetts.

3. J. Capon and N. R. Goodman, "Probability Distributions for Estimators of the Frequency Wavenumber Spectrum," Proc. IEEE, Vol. 58, October 1970.

4. N. R. Goodman, "Statistical Analysis Based on a Certain Multivariate Complex Gaussian Distribution," Annals of Mathematical Statistics, Vol. 34, March 1963.

5. P. L. Odell and A. H. Feiveson, "A Numerical Procedure to Generate a Sample Covariance Matrix," JASA, Vol. 61, 1966.

6. R. L. Fante, E. C. Barile, and T. P. Guella, "Clutter Covariance Smoothing by Subaperture Averaging," IEEE Transactions on Aerospace and Electronic Systems, Vol. 30, N0. 3, July 1994.

7. W. F. Gabriel, "Spectral Analysis and Adaptive Array Superresolution Techniques," Proc. IEEE, Vol. 68, June 1980.

8. J. Ward, "Space-Time Adaptive Processing for Airborne Radar," Lincoln Laboratory Technical Report 1015, 13 December 1994.